energies

MDPI

Article

On-Road and Laboratory Emissions from Three Gasoline Plug-In Hybrid Vehicles-Part 2: Solid Particle Number Emissions

Anastasios Melas *, Tommaso Selleri, Jacopo Franzetti, Christian Ferrarese, Ricardo Suarez-Bertoa and Barouch Giechaskiel *

European Commission, Joint Research Centre (JRC), 21027 Ispra, Italy; tommaso.selleri@eea.europa.eu (T.S.); jacopo.franzetti@ec.europa.eu (J.F.); christian.ferrarese@ec.europa.eu (C.F.); ricardo.suarez-bertoa@ec.europa.eu (R.S.-B.)

* Correspondence: anastasios.melas@ec.europa.eu (A.M.); barouch.giechaskiel@ec.europa.eu (B.G.)

Abstract: Plug-in hybrid electric vehicles (PHEVs) are a promising technology for reducing the tailpipe emissions of CO_2 as well as air pollutants, especially in urban environments. However, several studies raise questions over their after-treatment exhaust efficiency when their internal combustion engine (ICE) ignites. The rationale is the high ICE load during the cold start in combination with the cold conditions of the after-treatment devices. In this study, we measured the solid particle number (SPN) emissions of two Euro 6d and one Euro 6d-TEMP gasoline direct injection (GDI) PHEVs (electric range 52–61 km) all equipped with a gasoline particulate filter, in the laboratory and on-road with different states of charge of the rechargeable electric energy storage system (REESS) and ambient temperatures. All vehicles met the regulation limits but it was observed that, even for fully charged REESS, when the ICE ignited SPN emissions were similar or even higher in some cases compared to the operation of these vehicles solely with their ICE (discharged REESS) and also when compared to conventional GDI vehicles. On-road SPN emission rate spikes during the first 30 s after a cold start were, on average, 2 to 15 times higher with charged compared to discharged REESS due to higher SPN concentrations and exhaust flow rates. For one vehicle in the laboratory under identical driving conditions, the ICE ignition at high load resulted in 10-times-higher SPN emission rate spikes at cold-start compared to hot-start. At −10 °C, for all tested vehicles, the ICE ignited at the beginning of the cycle even when the REESS was fully charged, and SPN emissions increased from 30% to 80% compared to the cycle at 23 °C in which the ICE ignited. The concentration of particles below 23 nm, which is the currently regulated lower particle size, was low (≤18%), showing that particles larger than 23 nm were mainly emitted irrespective of cold or hot engine operation and ambient temperature.

Keywords: electric motor; gasoline direct injection; WLTC; RDE; cold-start emissions; sub-23 nm particles; REESS; low ambient temperature; hybrid vehicles; gasoline particulate filter

check for updates

Citation: Melas, A.; Selleri, T.; Franzetti, J.; Ferrarese, C.; Suarez-Bertoa, R.; Giechaskiel, B. On-Road and Laboratory Emissions from Three Gasoline Plug-In Hybrid Vehicles-Part 2: Solid Particle Number Emissions. *Energies* **2022**, *15*, 5266. https://doi.org/10.3390/en15145266

Academic Editors: Syu-Ruei Jhang and Sheng-Lun Lin

Received: 15 June 2022
Accepted: 18 July 2022
Published: 20 July 2022

1. Introduction

Road transport is an important contributor of greenhouse gases [1] that are responsible for global warming. Global CO_2 abatement goals have urged the electrification of vehicles that aims to carbon-free tailpipe emissions [2]. Life-cycle assessment studies on electric vehicles show potential benefits compared to conventional vehicles, especially if the technology change is combined with a low-carbon electricity mix [3–5]. The transition to purely electric vehicles (PEVs) is on-going; however, due to some barriers (e.g., short driving range, high cost) for their wide diffusion [6], also hybrid (the combination of an internal combustion engine and an electric motor) solutions are followed. Already since the late 1990s, the first hybrid electric vehicles (HEVs) were introduced in the market, while in the late 2000s, the first plug-in hybrid vehicles (PHEVs) were commercialized.

HEVs are equipped with an internal combustion engine and a rechargeable electric energy storage system (REESS) (i.e., battery) that captures energy during braking, stores it, and powers the vehicle. PHEVs (also referred as off-vehicle charge hybrid electric vehicles, OVC-HEVs, in the European regulation 2017/1151) can also externally charge the REESS, giving a higher electric range and minimizing the use of the ICE. The market share of commercial and passenger PHEVs has increased over the last few years [7]. Due to their extended electric operation, PHEVs have been expected to reduce tailpipe greenhouse gas emissions compared to conventional vehicles and also improve urban air quality.

However, different studies have identified a significant gap between official type approval and real-world CO_2 emissions of PHEVs which can be attributed to usage and charging behavior [8,9]. A recent study [10] showed that even if PHEVs emit lower CO_2 compared to conventional vehicles, the in-use CO_2 emissions are 1.5 to 2 times more than the official declared values. The impact of the user-selectable mode on the CO_2 variability of three PHEVs was also investigated in one study [11] and it was found that, when the discharged REESS was charged by the ICE, the CO_2 emissions were 50 to 100% higher than a trip with the REESS simply discharged. In another study [12], the cabin air-heating system and lower ambient temperatures were found to increase CO_2 emissions of two PHEVs. The higher real-world CO_2 emissions compared to official type approval values were attributed to the more frequent than expected ignitions of the ICE. This difference may also create implications for air pollutants.

PHEVs are frequently combined with a gasoline direct injection (GDI) engine. GDIs are known for improving fuel efficiency but may emit a higher solid particle number (SPN) compared to a port fuel injection (PFI) engine [13]. The high SPN emissions of GDIs have been handled in the European regulation by introducing a SPN limit down to a 23 nm particle size (SPN_{23}) in Euro 6 [14]. The regulation limit, also applicable to on-road testing, drove to the optimization of GDIs operation [15] and to the implementation of gasoline particulate filters (GPFs) which can efficiently reduce SPN emissions [16,17] with a trapping efficiency even >90% [18]. GDIs still emit high SPN concentrations during cold start, and the speed, load, or fuel/air ratio increase [19] but also during GPF regeneration [20]. Moreover, when the GPF is cold, its efficiency may be reduced [21]. Considering that PHEVs cold ICE ignition may occur under high power demand accelerations and with cold GPF, it is very likely that SPN emissions will be high.

SPN emissions of HEVs during engine ignitions and re-ignitions have been investigated by different studies. The on-road SPN emissions of two China-6 vehicles, a GDI-HEV and a PFI-HEV, both without gasoline particulate filter, were $>10^{12}$ #/km [22]. The SPN spikes corresponded to engine start events. The contribution of high instantaneous SPN emissions was assessed in a study [23] and it was found that, for three GDI-HEVs and one PFI-HEV, 20% of SPN was emitted in 2% of driving time. Another study compared the SPN emission rate (#/s) of a 2012 light-duty gasoline HEV during re-ignition events and found that they were 2.5 to 4.4 higher compared to stabilized ICE conditions [24]. In another study [25], the SPN emissions of a 2019 HEV with GDI during ICE re-ignitions accounted for ~70% of total trip SPN. A combination of injection pressure, end of injection, and spark timing modifications reduced ICE re-ignition SPN emissions by ~88%.

Few researchers have studied the SPN emissions of PHEVs. A study that measured real-driving SPN emissions of a Euro 6b PHEV equipped with a GDI engine [26] found that SPN emissions were higher in the hybrid mode compared to ICE-dominant trips in the highway, whilst fuel consumption was lower. Researchers [27] measured the particle sizes during the first cold engine ignition in laboratory cycles and observed that accumulation particles were mainly emitted. Cold-start SPN emissions were attributed to the fuel combustion and not to the oil. The high SPN emissions during ICE ignitions, especially at trips with fully or partially charged REESS, were confirmed by others as well [28], and the authors claimed that optimization of GPFs will be needed to achieve stricter regulation limits. A comparison between a GDI and a PHEV with GDI, both equipped with a GPF, showed that similar soot management can be also applied to PHEVs, but calibration should be performed at high states of charge (SOCs) of the REESS to avoid high GPF inlet temperature [29].

In this study, we investigate SPN emissions of three Euro 6 PHEVs with a GDI engine equipped with a GPF. The gaseous emissions have been published in a companion paper [11]. SPN_{23} emission factors are presented for laboratory tests performed according to the worldwide harmonized light vehicles test procedure (WLTP) and on-road tests with variable REESS states of charge (SOCs). The variability of SPN emissions at different SOCs are determined and the effect of cold ICE ignitions at trips with charged or partially charged REESS is compared to ICE-dominant trips. Furthermore, the ambient temperature effect on SPN_{23} is studied. Finally, the sub-23 nm particles emissions as well as their contribution to SPN are presented.

2. Materials and Methods

The following subsections describe the plug-in hybrid vehicles that were tested, the laboratory and on-road driving cycles and protocols, and the instrumentation used for SPN measurements.

2.1. Vehicles

Table 1 summarizes the main characteristics of the tested vehicles. Vehicles are denoted with Vx, where x is their number. The number was selected according to the chronological order in which the vehicles were tested. All of them were PHEVs equipped with a GDI engine. Their class was M1 (passenger cars) and the model year was 2020. The after-treatment devices were a three-way catalyst (TWC) and a GPF. V1 and V3 were type-approved as Euro 6d, while V2 was type-approved as Euro 6d-TEMP. Thus, for all of them, a SPN_{23} limit of 6×10^{11} #/km was applicable at type-approval laboratory tests and the not-to-exceed (NTE) limit of 9×10^{11} #/km on the road (i.e., with a conformity factor of 1.5). Moreover, all vehicles had to fulfil the in-service conformity tests (ISC), meaning that they should comply with emission limits up to 100,000 km or 5 years, whichever comes first. V1 and V2 had low mileage (~3000 km), while V3 had ~14,000 km. V1 and V3 had identical characteristics of thermal engine and electric motor, but were commercialized by different manufacturers and had different mileage. Moreover, their test mass was slightly different. V2 had lower test mass, engine displacement (1499 vs. 1598 cm^3), power (100 vs. 133 kW), electric range (52 vs. 61 km), and declared SPN_{23} (1.29×10^{11} vs. 1.86×10^{11} #/km) compared to V1 and V3. The engine displacement, power, electric range, and declared SPN_{23} under charge-sustaining conditions are reported in Table 1. All vehicles were maintained according to the requirements of the manufacturer. Commercial gasoline fuel E10 was used for testing.

Table 1. Main characteristics of tested vehicles.

Specification	V1	V2	V3
Class	M1	M1	M1
Propulsion type	PHEV	PHEV	PHEV
Fuel	Gasoline	Gasoline	Gasoline
Injection	Direct Injection	Direct Injection	Direct Injection
ATS	TWC, GPF	TWC, GPF	TWC, GPF
Euro	6d-ISC	6d-TEMP-EVAP-ISC	6d-ISC
Year	2020	2020	2020
Mileage	3092	2977	14,360
Test mass (kg)	1867	1779	1882
Engine displacement (cm^3)	1598	1499	1598
Power (kW)	133	100	133
Electric range (km)	61	52	61
Declared SPN_{23} (#/km)	1.86×10^{11}	1.29×10^{11}	1.86×10^{11}

ATS = after-treatment system; EVAP = evaporative emissions; GPF = gasoline particulate filter; ISC = In-service conformity; PHEV = plug-in hybrid electric vehicle; SPN_{23} = solid particle number down to 23 nm; TWC = three-way catalyst.

2.2. Driving Cycles and Routes

In Europe, light duty vehicles are tested according to Regulation 2017/1151. For internal combustion engine-equipped vehicles, the worldwide harmonized light vehicles test cycle (WLTC) applies. This driving cycle is performed at 23 °C, it consists of low, medium, high, and extra high speed phases, while its total duration is 1800 s. More information can be found elsewhere [30].

PHEVs, in addition to testing with depleted REESS (charge-sustaining conditions), have to also be tested with charged REESS (charge-depleting conditions). Their testing consists of a series WLTC, and four different options for the order of tests are prescribed in 2017/1151. Herein, we applied option three. Accordingly, a preconditioning WLTC was conducted under charge-sustaining conditions. Then, the vehicle was soaked at 23 °C for ~20 h and the REESS was fully charged. Subsequently, a series of charge-depleting (CD) WLTC cycles were performed until the break-off criterion was fulfilled. The break-off criterion is reached when the relative change in the REESS at consequent cycles is less than 4%. The WLTC in which this criterion is reached is called the confirmation cycle, while the previous one is called the transition cycle. The maximum soaking time between CD cycles was 30 min, while the REESS was not charged. After the completion of the CD cycles, the vehicle was soaked for ~20 h and then a charge-sustaining (CS) WLTC was performed. The REESS current and voltage were continuously measured during the tests. According to the regulation, the weighted emissions of a PHEV are calculated by considering the CD cycles until the transition WLTC and the CS WLTC. SPN_{23} emissions of these cycles are weighted using the utility factors described in 2017/1151. Fractional utility factors apply for each phase and depend on the travelled distance. According to this method, the first driven cycle has a larger weight on the total emissions calculation compared to the subsequent ones (~50% in our case). In addition to WLTC testing at 23 °C, all vehicles were tested both with CD and CS tests at −10 °C. Moreover, V2 and V3 were also tested only with CS at 40 °C.

For on-road testing, there is no provision in the European real driving emissions (RDE) regulation, consolidated in 2017/1151, for the state of charge (SOC) of PHEVs. Thus, a PHEV should comply with the RDE regulation requirements under all different SOC levels. Herein, we conducted RDE-compliant tests with different SOC (100%, 50%, 25%, discharged). For some SOCs, more than one test was performed. The trip duration was ~103 min and was composed of an urban (~35.5 km), a rural (~29.1 km), and a highway (~26.5 km) section according to the regulation requirements. Note that the limits apply both to the urban and to the total trip SPN_{23} emissions. The vehicles were tested in different months; thus, the ambient temperature varied. The average trip temperatures were 8 to 18 °C for V1, 25 to 32 °C for V2, and 19 to 28 °C for V3. All tests were carried out with the default driving mode, except from two tests of V1 which were performed in the electric user-selectable mode (indicated in the "Results and Discussion" section).

Table 2 presents all laboratory and on-road tests performed for each vehicle.

Table 2. Summary of laboratory and on-road tests.

Specification	State of Charge	V1	V2	V3
WLTC 23 °C	Charge-depleting Charge-sustaining	Yes Yes	Yes Yes	Yes Yes
WLTC −10 °C	Charge-depleting Charge-sustaining	Yes Yes	Yes Yes	Yes Yes
WLTC 40 °C	Charge-sustaining	No	Yes	Yes
RDE	Charge-depleting * Charge-sustaining	Yes Yes	Yes Yes	Yes Yes
RDE temperature	-	8–18 °C	25–32 °C	19–28 °C

* Charge-depleting RDE tests were performed with a 100%, 50%, and 25% state of charge. WLTC = worldwide harmonized light vehicles test cycle. RDE = real driving emissions.

2.3. Instrumentation

Laboratory tests were conducted at the vehicle emissions laboratory (VELA 8) of the Joint Research Centre in Italy. VELA 8 is a climatic test cell equipped with a 4WD chassis dynamometer. SPN_{23} was measured from a dilution tunnel with constant volume sampling (CVS). The particle counter was the APC 489 from AVL (Graz, Austria) [31]. It consisted of a hot dilution stage at 150 °C, an evaporation tube at 350 °C, a cold dilution stage, and a particle counter with a cut-off size at 23 nm. Additionally, a particle counter with cut-off size down to 10 nm was used for measuring SPN_{10}. The dilution factor combined with the particle losses through the APC 489, were expressed through the particle number concentration reduction factor (PCRF). Due to the high SPN emissions of PHEVs during their cold start, we used PCRF = 1000 in order to avoid saturation of the particle number counter and minimize volatile artifacts in the system [32].

On-road testing was performed with two different portable emissions measurement systems (PEMS), namely an AVL MOVE system (for V1 and V3) and a HORIBA (Kyoto, Japan) OBS ONE system (for V2). MOVE utilizes a particle detector based on diffusion charging technology, while the OBS particle detector is based on condensation particle counting. The cut-off size of PN-PEMS systems was 23 nm. In parallel with these two PEMS, a portable Fourier transform infrared (FTIR) spectrometer was also installed on the vehicles. More information can be found in the companion paper of this work [11].

Note that all instrumentation used in this study was maintained and calibrated according to the regulation requirements. The estimated measurement uncertainty is around 14% for the laboratory system and 31% for the portable system. A detailed discussion on the uncertainty of regulatory SPN measurements in the laboratory and on-road can be found in [33].

3. Results and Discussion

In this section, we present the SPN_{23} emissions of V1 to V3 under regulated laboratory (3.1) and on-road (3.2) tests, we determine the emission rate and concentration SPN_{23} spikes during on-road cold engine ignition of the ICE (3.3), we investigate the effect of low- (-10 °C) and high-temperature (40 °C) tests in the laboratory (3.4), and finally we present the SPN_{10} emissions measured in laboratory tests for V1 and V2 (3.5).

3.1. Regulated Laboratory Tests

Figure 1 presents the SPN_{23} emissions of the three plug-in vehicles (V1 to V3) measured in the laboratory when tested with the type-approval WLTC. Only testing cycles for which the ICE ignited are shown. All vehicles were powered exclusively with the electric motor for the first two charge-depleting cycles (CD1 and CD2) and during the third CD (CD3) the ICE ignited for the first time. SPN_{23} emissions during CD3 are presented with blue and white diagonal lines and the charge-sustaining (CS) emissions are presented with an orange bar with grid. Additionally, the weighted WLTP SPN_{23} emissions, calculated according to 2017/1151, are plotted with a grey bar. The red dashed line shows the Euro 6 SPN_{23} limit (6×10^{11} #/km) and the black dotted line shows the average SPN_{23} emissions of all GDI vehicles, equipped solely with an internal combustion engine (6.3×10^{10} #/km), tested during the 2020–2021 market surveillance activities of the Joint Research Centre (JRC), and specifically of six Euro 6d-TEMP and two Euro 6d, all equipped with GPF [34].

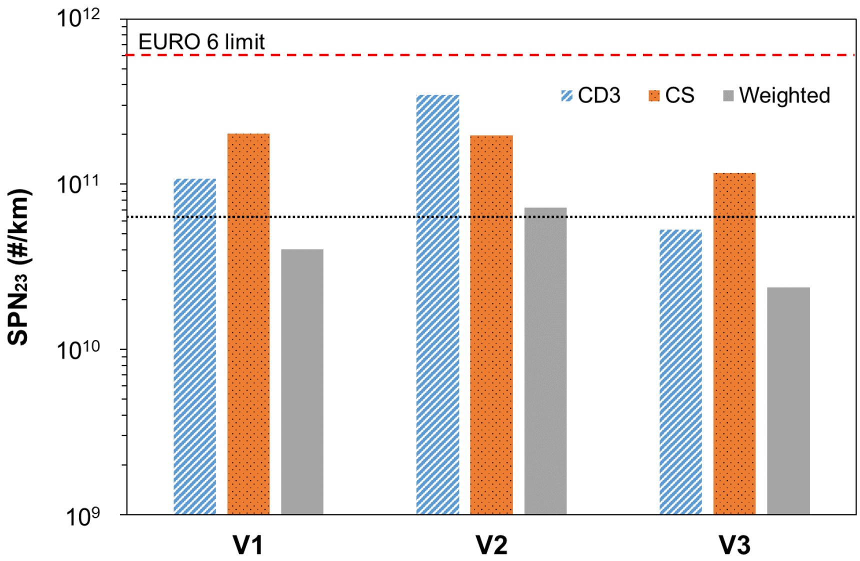

Figure 1. Solid particle number emissions (>23 nm) (SPN_{23}) of three plug-in hybrid electric vehicles (V1 to V3) at the Type 1 test WLTC during charge-depleting (CD) and charge-sustaining (CS) rechargeable electric energy storage (REESS) conditions as well as the weighted SPN_{23} emissions considering the electric range calculated according the regulation 2017/1151. The internal combustion engine (ICE) ignited for first time during the third consecutive CD cycle (CD3) for all vehicles. In CD1 and CD2, the vehicle was powered only by the electric motor and these cycles were not plotted as SPN_{23} (#/km) was zero. The red dashed line shows the Euro 6 limit (6×10^{11} #/km) and the black dotted line shows the average WLTC SPN_{23} emissions of eight conventional Euro 6d/6d-TEMP gasoline direct injection vehicles [34].

All vehicles complied with the Euro 6 limit. Note that when testing a PHEV, the limit has to be respected at all cycles (both CD and CS). V1 emitted ~1×10^{11} #/km during CD3 and approximately two times more (~2×10^{11} #/km) during the CS WLTC. Also for V3, the CS emissions were almost double compared to the CD3 emissions (1.2×10^{11} #/km vs 5.3×10^{10} #/km, respectively). On the contrary, V2 emitted higher SPN_{23} during CD3 (3.5×10^{11} #/km) compared to CS (2.0×10^{11} #/km) even if the ICE operated for ~880 s during CD3.

SPN_{23} emissions during CS cycles were higher than the average of the eight GDI vehicles presented in Figure 1. This result shows that PHEVs, when operating solely with the ICE, perform equally or even worse than conventional vehicles with regards to particulate emissions, possibly due to their larger weight related to the additional REESS weight. A previous study found that payload may increase SPN emissions [35]. CD3 emissions of V1 and V2 were higher than the average of conventional GDIs, while for V3 lower. The weighted emissions were $\leq 7.2 \times 10^{10}$ #/km for all vehicles and lower (V1 and V3) or equal (V2) to conventional Euro 6d/6d-TEMP GDIs.

To better understand the SPN_{23} emissions of V2 during CD3 and CS, we plotted the cumulative SPN_{23} emissions over time in Figure 2a. We also plotted the ICE speed (rpm) during the two tests. During the CS, the ICE switched on a few seconds after the initiation of the cycle and powered the vehicle until ~300 s. Then, it remained off almost always until 635 s when it re-ignited. During the first 40 s after the ICE ignition, cumulative SPN_{23} steeply increased up to ~7×10^{11} # which corresponded to ~16% of the particles emitted during the entire cycle (4.5×10^{12} #). After 40 s, the cumulative SPN_{23} slope changed and it continuously increased during the test cycle.

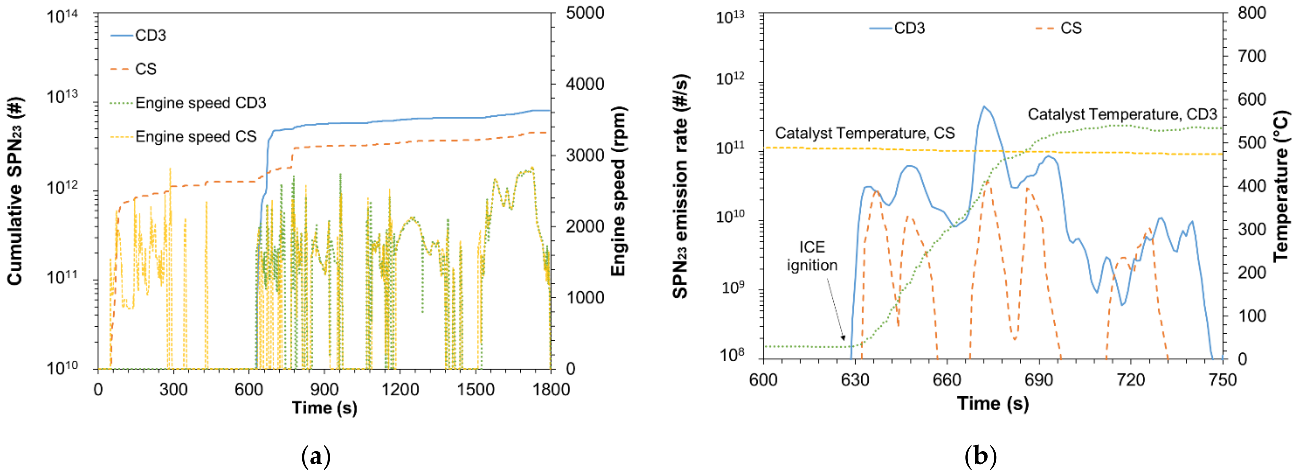

(**a**) (**b**)

Figure 2. SPN_{23} (**a**) cumulative (#) and (**b**) emission rate (#/s) emissions and of V2 over time, during the third charge-depleting (CD3) WLTC and the charge-sustaining cycle (CS) WLTC.

During CD3, ICE switched on after ~630 s and powered the vehicle (as already reported above) for total ~880 s. Cumulative SPN_{23} steeply increased during the first 70 s after the cold start and ~4.8×10^{12} # was emitted which corresponded to ~60% of the total cycle SPN_{23}. Note that in the entire CS, the total SPN_{23} emitted was 4.5×10^{12} #. In order to put this result in the right context, considering the limit of 6×10^{11} #/km, the SPN_{23} during a WLTC could not overcome ~1.4×10^{13} #. Thus, V2 emitted ~32% of the maximum cumulative SPN_{23} (#) permitted during a WLTC in 70 s, covering a distance of 650 m. Whilst SPN_{23} emissions were below the regulation limits, their spatial distribution was non-uniform in this case.

Figure 2b plots the SPN_{23} emission rate of V2 during CD3 and CS. We focus on the time frame in which the ICE ignited for the first time in CD3 and re-ignited in CS. We also plot the catalyst temperature which was obtained by the on-board diagnostics system. There was no information on the exact position of the temperature sensor (i.e., before or after the GPF); therefore, its signal was used as a qualitative indication of the exhaust after-treatment system (ATS) condition (cold or hot). As already mentioned, the ICE ignited after ~635 s. In CD3, the after-treatment and the ICE were cold, while in CS they were hot. The SPN_{23} emission rate spikes in CD3 were even 10 times higher compared to CS. Considering that the test cycle was identical, the emission rate spike difference may be attributed to higher SPN_{23} concentrations and not to significant exhaust flow differences (note that emission rate depends on the concentration and the exhaust flow).

3.2. Regulated On-Road Tests

On-road tests were performed according to the European RDE regulation, consolidated in 2017/1151. The vehicles were tested with different REESS SOCs, i.e., fully charged (CD100), 50% charged REESS (CD50), 25% charged REESS (CD25), and discharged REESS (CS). Soaking was performed in the laboratory at around 20 °C, while in one case for V1, soaking was performed outside at around 3 °C. Figure 3 plots the SPN_{23} (#/km) emissions during the entire trip that consisted of an urban, a rural, and a highway part (total distance around 91 km). The black dotted line indicates the average on-road SPN_{23} emissions of all Euro 6d/6d-TEMP GDI vehicles (7.8×10^{10} #/km) tested in the period 2020–2021 in the framework of JRC market surveillance activities [34]. The red dashed line depicts the on-road NTE limit of 9×10^{11} (#/km). Error bars show the maximum and minimum measured values for tests where more than one repetition was performed. All tests were performed with the default user-selectable mode, except for two tests of V1 (CD100 soak out and CD50) which were conducted with the user-selectable electric mode.

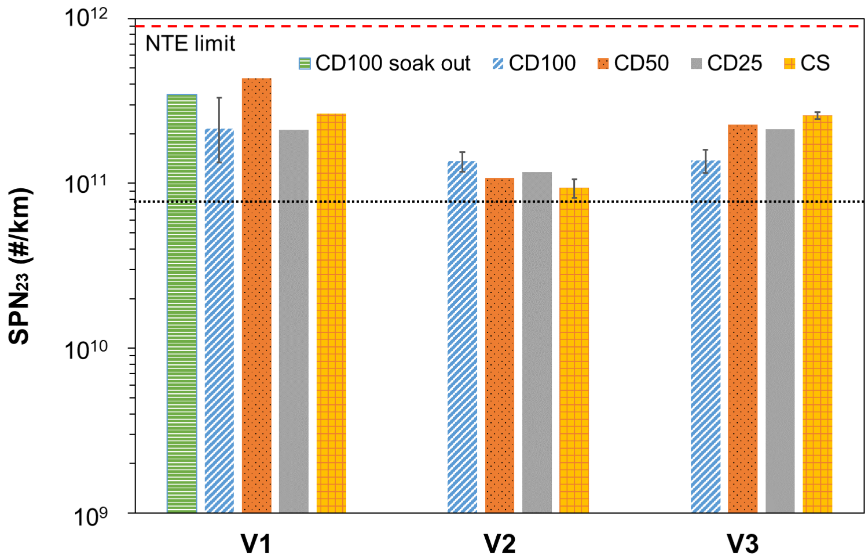

Figure 3. Solid particle number emissions (>23 nm) (SPN_{23}) of three plug-in hybrid electric vehicles (V1 to V3) during on-road tests performed according to the European real driving emissions regulation (RDE4). CDx denotes the charge of the REESS; CD100 for 100%, CD50 for 50%, CD25 for 25%. CS stands for trips in charge-sustaining or discharged REESS. The error bars show the maximum and minimum values for tests with more than one repetition. The red dashed line shows the Euro 6 on-road not-to-exceed (NTE) limit (9×10^{11} #/km) and the black dotted line shows the average on-road SPN_{23} emissions of eight conventional Euro 6d/6d-TEMP gasoline direct injection vehicles [34].

All vehicles under all conditions complied with the NTE limit, but in all cases SPN_{23} emissions of the tested vehicles were higher than the average values observed for conventional vehicles. V1 emitted the highest SPN_{23} (1.3×10^{11}–4.3×10^{11} #/km), while V2 emitted the lowest (8.1×10^{10}–1.1×10^{11} #/km). For V1, the test with the highest emissions was CD50, while for V3 the test with the highest emissions was CS. Interestingly, for V2, the test with the highest emissions was for fully charged REESS (CD100). Soaking out at an average ambient temperature of 3 °C resulted an increase in SPN_{23} emissions. In summary, the particle emissions did not benefit from charged REESS, but in some cases the emissions were higher in this trip of ~91 km even with fully charged REESS. This finding is in agreement with previous studies [26,28] which found that the high-load cold-start emissions of PHEVs may dominate the total SPN_{23} emissions.

Figure 4 plots the SPN_{23} emissions during the urban part of the trip (distance of approximately 35.5 km). Note that, according to RDE, the NTE limit also applies to the urban section (red dashed line). Similar to Figures 1 and 3, the average values of conventional vehicles are plotted with a black dotted line (6.5×10^{10} #/km). Also in this case all vehicles complied with the limits while only V2 and V3 with fully charged REESS emitted less than the conventional vehicles. For V3, as the REESS SOC decreased, the vehicle emitted more particles. In contrast, for V1 and V2, SPN_{23} emissions varied and no relation with REESS SOC was found, except from CD100 where the emissions were lower than CD50, CD25, and CS. This is related to the fact that the electric range of the tested vehicles was higher than the distance travelled in the urban environment and the ICE was on only for short distances. It should be highlighted that even for short urban trips, shorter than the electric range of the vehicles, the ICE ignited producing a significant amount of particles.

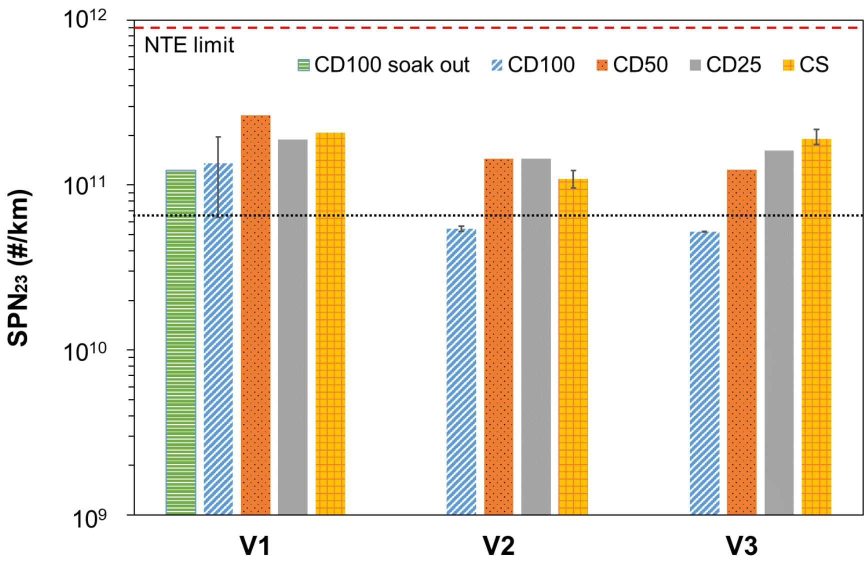

Figure 4. Solid particle number emissions (>23 nm) (SPN_{23}) of three plug-in hybrid electric vehicles (V1 to V3) during the urban part of on-road tests performed according to the European real driving emissions regulation (RDE4). CDx denotes the charge of the REESS; CD100 for 100%, CD50 for 50%, CD25 for 25%. CS stands for trips in charge-sustaining or discharged REESS. The error bars show the maximum and minimum values for tests with more than one repetition. The red dashed line shows the Euro 6 on-road not-to-exceed (NTE) limit (9×10^{11} #/km) and the black dotted line shows the average urban on-road SPN_{23} emissions of eight conventional Euro 6d/6d-TEMP gasoline direct injection vehicles [34].

Next, we focus on the SPN_{23} emissions of V2 presented in Figure 3. As already discussed, with fully charged REESS, the vehicle emitted the highest SPN_{23}. Figure 5 plots the cumulative SPN_{23} emissions against distance. The red dashed line depicts the not-to-exceed cumulative SPN_{23}, according to the distance travelled by the vehicles. The tests CD100 and CS had two or more repetitions. In order to examine the best case scenario for the impact of cold-start emissions, we plotted the CD100 test with the lowest emissions and the CS with the highest emissions in Figure 5. When the REESS was discharged, the ICE ignited at the beginning of the trip. The ICE ignition during the CD cycles occurred after ~8, ~21, and ~40 km for CD25, CD50, and CD100, respectively. In maximum 3 km after the ICE ignition, the same amount of cumulative SPN_{23} was emitted as in the CS trip until this distance. During the first 1 km in CS, V2 emitted 19% of the total trip emissions, while in CD100 it emitted 22%. In all cases, except for CD25, during the first kilometer after the ICE cold start more than 2×10^{12} # were emitted. The strong effect of the high-load cold start resulted in high particle concentration emissions. In the charge-depleting cycles, the maximum spike concentrations during cold start were 1.3×10^7 (#/cm^3), 1.5×10^7 (#/cm^3), and 1.7×10^7 (#/cm^3) for CD100, CD50, and CD25, respectively, while during the CS trip they were 5×10^6 (#/cm^3).

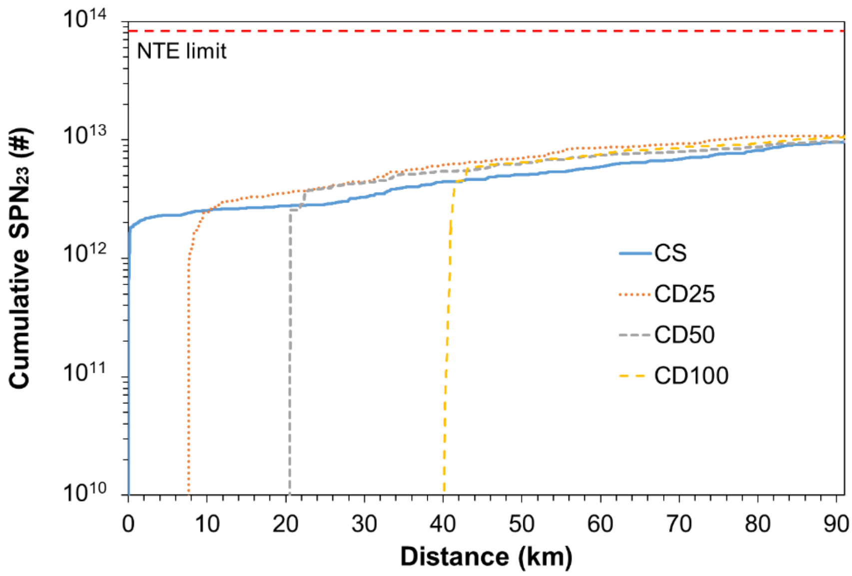

Figure 5. Cumulative SPN_{23} emissions of V2 over distance, tested on-road according to the European real driving emissions regulation (RDE). CDx denotes the charge of the REESS; CD100 for 100%, CD50 for 50%, CD25 for 25%. CS stands for trips in charge-sustaining or discharged REESS. The red dashed line shows the Euro 6 on-road not-to-exceed (NTE) limit multiplied with the distance driven.

Another important aspect of on-road tests of PHEVs is the variability of SPN_{23} emissions due to different REESS testing conditions. We calculated the coefficient of variation (i.e., the ratio of the standard deviation to the mean) of SPN_{23} emissions considering the average emissions of each testing condition; CD100 (not soak out), CD50, CD25, CS. In overall, urban emissions exhibited highest variance especially for V2 (38%) and V3 (45%). For V1, also total SPN_{23} emissions varied significantly and namely 37%. In a previous study, the variability of SPN_{23} emissions emitted by a GDI engine under a simulated RDE trip (well-controlled conditions) was found to be 22% [36]. The difference with our findings is small considering in our case the variability of traffic and ambient temperature conditions as well as the different conditions during the ICE ignition. Table 3 summarizes the coefficient of variation of SPN_{23} emissions under on-road tests performed in this study.

Table 3. Coefficient of variation of SPN_{23} emissions under the on-road tests with four different REESS states of charge, i.e., 100%, 50%, 25%, and discharged REESS.

	Route Section	V1	V2	V3
Coefficient of variation	Urban	27%	38%	45%
	Total	37%	16%	24%

3.3. Emissions at Cold Engine Ignitions

The highest SPN_{23} emission rate spike (#/s) during ICE cold start (considering the first ~30 s after the first ICE ignition) at each test was determined and then averaged over all charge-depleting and charge-sustaining on-road tests. Figure 6a presents the average values for the tested vehicles and the error bars show the maximum and minimum value. Note that in ~65% of CD trips, the ICE ignited in the urban environment. SPN_{23} emission rate spikes in CD were, on average, ~3.5, ~15, and ~2 times higher than in CS for V1, V2, and V3, respectively. In order to exclude the exhaust flow rate effect, we plot the average of the highest SPN_{23} concentration (#/cm^3) spikes in Figure 6b. For V1 and V2, the concentration spikes are approximately three times higher during CD trips compared to CS. Instead, for V3, the spikes during CS were approximately 1.5 times higher compared to CD and the cold-start effect during high load was smaller. Thus, for V1, higher SPN_{23} emission rates were due to higher SPN_{23} concentrations; for V2, it was a combination of exhaust flow and concentration; and for V3, it was due to higher exhaust flow rates. Note that the cold-start concentrations of PHEVs reached approximately 2×10^7 #/cm^3 and these high concentration levels should be taken into consideration when designing SPN_{23} measurement instruments in order to ensure high accuracy and avoid the saturation of SPN detectors.

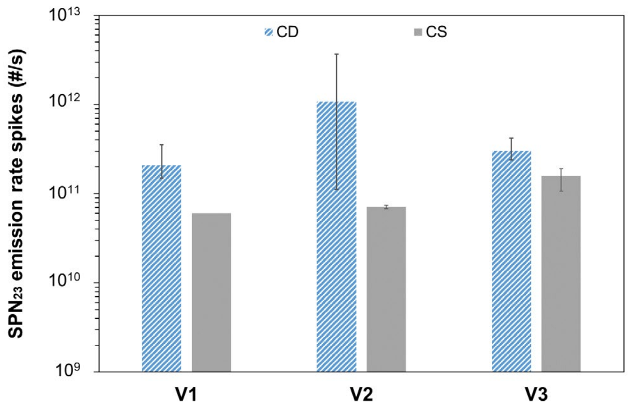

(**a**)

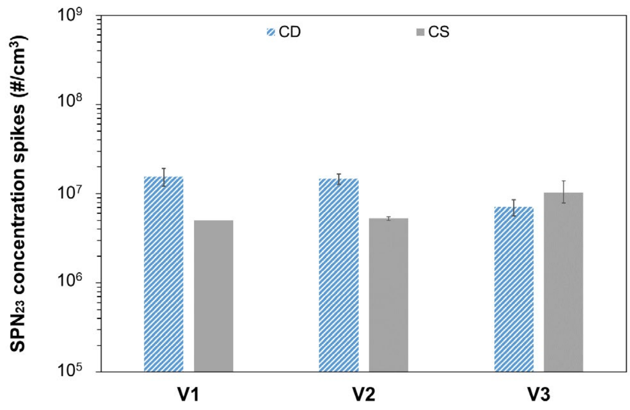

(**b**)

Figure 6. SPN_{23} (**a**) emission rate (#/s) and (**b**) concentration (#/cm^3) spikes at on-road tests during the cold start of the internal combustion engine. CD stands for charge-depleting tests and CS stands for charge-sustaining tests. The error bars depict the maximum and minimum values.

3.4. Temperature Effect

The WLTC CD and CS regulatory cycles were also performed at −10 °C. For V2 and V3, a high-temperature (40 °C) test was also done in CS. Note that these two temperatures were outside the boundaries of on-road testing and no SPN limit was applicable. Figure 7a plots the SPN_{23} (#/km) emissions during the CD cycle in which the ICE ignited for the first time and Figure 7b plots emissions during the CS cycles. In both figures, the emissions at 23 °C were also plotted (presented in Figure 1). The dashed red lines indicate the Euro 6 regulation limit at cycles in which it is applicable.

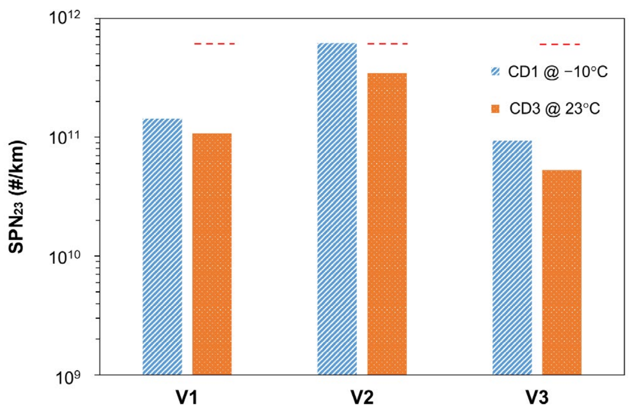

(**a**)

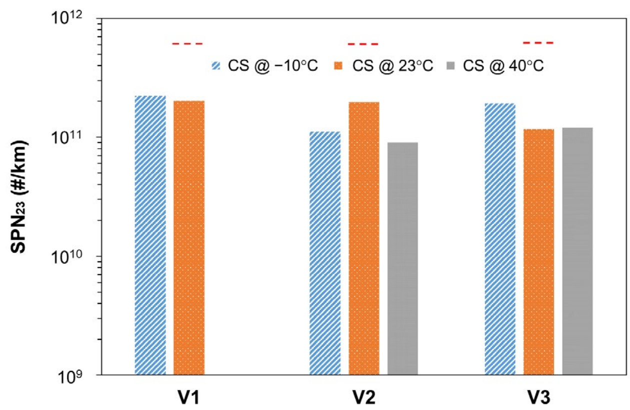

(**b**)

Figure 7. Solid particle number emissions (>23 nm) (SPN_{23}) of three plug-in hybrid electric vehicles (V1 to V3) over the WLTC at different temperatures and during (**a**) charge-depleting (CD) and (**b**) charge-sustaining (CS) rechargeable electric energy storage (REESS) conditions. Only CD cycles in which the internal combustion engine was ignited for the first time are plotted. The red dashed lines indicate the Euro 6 limit (6×10^{11} #/km) for the tests in which it was applicable.

For all tested vehicles, at −10 °C and with fully charged REESS, the ICE ignited during the first CD cycle (CD1) and specifically at the beginning of the test. SPN_{23} emissions were higher compared to CD3 at 23 °C and specifically from ~30% for V1 to ~80% for V2. For V2, SPN_{23} at −10 °C was slightly higher than the limit (6.2 × 10^{11} #/km). Although the limit does not apply at this extreme temperature, we should also consider that these SPN_{23} emissions corresponded to a fully charged PHEV.

For CS cycles, the temperature effect was not so clear. Indeed, for V2, the highest SPN_{23} emissions were measured at 23 °C, while for V1 and V3 they were measured at −10 °C. At 40 °C, the SPN_{23} emissions were lower (V2) or equal (V3) to 23 °C. In all cases, the SPN_{23} emissions were below the emission limit which applies at 23 °C. This result is in agreement with a previous study that observed high GPF effectiveness at a temperature range from −30 °C to 50 °C [21].

3.5. Sub-23 nm Particle Emissions

In addition to SPN_{23}, SPN_{10} was also measured for V1 and V2 during laboratory tests at −10 °C and 23 °C. Table 4 presents the SPN_{23}, SPN_{10}, and the sub-23 nm particles contribution calculated by $(SPN_{10} - SPN_{23})/SPN_{23}$. The sub-23 nm contribution was lower than 20% in all cases. GDI engines may emit particles from 10 to 40 nm, especially under high-load transients, but the introduction of GPFs can effectively reduce these small-size particles [37]. In this study, the low sub-23 nm contribution may be attributed either to the efficiency of the GPFs and/or to the larger size of particles generated during the cold-start emissions which dominate the SPN of the entire test.

Table 4. Contribution of sub-23 nm particles, $(SPN_{10}\text{-}SPN_{23})/SPN_{23}$, at different laboratory cycles of V1 and V2.

Vehicle	WLTC	Temperature (°C)	SPN_{23} (#/km)	SPN_{10} (#/km)	Sub-23 nm Contribution
V1	CD3	23	1.08×10^{11}	1.15×10^{11}	7%
	CS	23	2.02×10^{11}	2.38×10^{11}	18%
	CD1	−10	1.43×10^{11}	1.54×10^{11}	9%
	CS	−10	2.22×10^{11}	2.36×10^{11}	7%
V2	CD3	23	3.47×10^{11}	3.85×10^{11}	11%
	CS	23	1.97×10^{11}	2.21×10^{11}	12%
	CD1	−10	6.21×10^{11}	6.63×10^{11}	7%
	CS	−10	1.11×10^{11}	1.22×10^{11}	10%

4. Conclusions

In this study, the SPN emissions of three PHEVs (V1 to V3) (electric range of 52–61 km), equipped with GDI engines, were studied in the laboratory and on-road. The laboratory test cycle was the regulated WLTC at different temperatures (−10 °C, 23 °C, and 40 °C), and also unregulated SPN_{10} was measured in some cases. On-road tests were performed according to the current RDE regulation (a total distance of ~90 km and an urban distance of ~35 km). The main focus was the effect of different REESS SOCs on the SPN_{23} emissions.

All vehicles complied with regulation limits, both in the laboratory and on-road, but their emissions compared to conventional vehicles equipped with GDI engines were either comparable or even higher in many cases. The rationale was that after the ignition of the ICE, any benefit, in terms of SPN emissions, from the electric motor operation was vanished in short periods (less than 70 s in one case) and driven distances (less than 1 km in one case). Even the weighted laboratory emissions calculated with utility factors applied for the weight of each testing cycle (larger weight to cycles with fully charged REESS) were higher than the average SPN_{23} of conventional vehicles for one of the tested vehicles of this study (V2). For on-road tests (a driven distance of ~90 km), the PHEVs emitted more SPN_{23} than the average of conventional GDIs, but exhibited better performance in terms of SPN_{23} for two out of three vehicles at urban environments when the REESS was fully charged. The variability of on-road SPN_{23} emissions was also studied for different REESS SOCs. For the total trip the variability ranged from 16% to 37% and in the urban section from 27% to 45%.

The effect of cold-engine starts on SPN_{23} emissions was investigated. In the laboratory, the SPN_{23} emission rate spikes (in #/s) during an ICE ignition at high load were approximately ten times higher at cold-start compared to hot-start under identical driving conditions. For on-road tests, the highest SPN_{23} emission rate spike after the first ICE ignition (considering the first 30 s) was determined and averaged for charge-depleting and charge-sustaining trips. It was shown that when the first ignition occurs during the trip, the cold-start SPN_{23} emission rate spikes can be 2 to 15 times higher than the spikes in charge-sustaining REESS where the engine ignites at the beginning of the trip. This difference was due to higher SPN_{23} concentrations (in #/cm^3) but also exhaust flow rates. For V1, the average cold-start emission rate spike differences between CD and CS trips were similar to cold-start SPN_{23} concentration spike differences and approximately three times higher in CD compared to CS. For V2, both the exhaust flow rate (approximately five times higher in CD cold start) and SPN_{23} concentrations (approximately three times higher in CD cold start) contributed to the 15-times-higher cold-start emission rate differences. For V3, the higher exhaust flow rate was mainly responsible for the SPN_{23} emission rate differences, as SPN_{23} concentration spikes were higher during cold start at CS on-road tests. The impact of the cold-start emissions was also supported by the contribution of 22% to total emissions in a trip with fully charged REESS. Cumulative cold-start emissions of V2 in the first km after the ICE ignition were $>2 \times 10^{12}$ #. Considering that approximately 65% of the cold starts occurred in the urban environment, special attention should be given to these high emission rates due to the highly non-uniform spatial distribution of PHEV SPN emissions. These results highlight the need for improvements in the combustion process during frequent cold starts or the implementation of high filtration efficiency filters at hybrid vehicles.

Low temperatures had a significant impact on the REESS operation. Specifically, even with fully charged REESS at -10 °C, the ICE ignited and emissions were 30% to 80% more than during the first charge-depleting cycle at 23 °C when the ICE ignited. In charge-sustaining cycles, the temperature did not have a strong effect. Finally, the sub-23 nm particles emitted by V1 and V2 were measured during laboratory tests (23 °C and -10 °C) and their contribution to SPN was low (<20% in all cases).

Author Contributions: Conceptualization, A.M. and T.S.; methodology, A.M. and B.G.; formal analysis, A.M., J.F., C.F., and T.S.; supervision, B.G. and R.S.-B.; writing—original draft preparation, A.M.; writing—review and editing, B.G., T.S., and R.S.-B. All authors have read and agreed to the published version of the manuscript.

Funding: This research received no external funding.

Institutional Review Board Statement: Not applicable.

Informed Consent Statement: Not applicable.

Data Availability Statement: Data is available upon request from the corresponding authors.

Acknowledgments: The authors would like to acknowledge the support and collaboration of M. Carriero, M. Otura, F. Forni, M. Centurelli, P. Canevari, P. Buchet, J.M. Crochemore, L. Bigozzi, A. Bonamin, and M. Stefanini.

Conflicts of Interest: The authors declare no conflict of interest.

Disclaimer: The opinions expressed in the manuscript are those of the authors and should in no way be considered to represent an official opinion of the European Commission. Mention of trade or commercial products does not constitute endorsement or recommendation by the authors or the European Commission.

Abbreviations

ATS	After-treatment system
CD	charge-depleting
CS	charge-sustaining
CVS	constant volume sampling
FTIR	Fourier transform infrared
GDI	gasoline direct injection
HEV	hybrid electric vehicle
ICE	internal combustion engine
ISC	in-service conformity
NTE	not-to-exceed
PCRF	particle number concentration reduction factor
PEMS	portable emissions measurement system
PEV	purely electric vehicle
PFI	port fuel injection
PHEV	plug-in hybrid vehicle
RDE	real driving emissions
REESS	rechargeable electric energy storage system
SOC	state of charge
SPN	solid particle number
TWC	three-way catalyst
WLTC	worldwide harmonized light vehicles test cycle
WLTP	worldwide harmonized light vehicles test procedure

References

1. European Environmental Agency. *The European Environment—State and Outlook 2020. Knowledge for Transition to a Sustainable Europe 2019*; European Environmental Agency: Copenhagen, Denmark, 2019. [CrossRef]
2. CO2 Emission Performance Standards for Cars and Vans. Available online: https://ec.europa.eu/clima/eu-action/european-green-deal/delivering-european-green-deal/co2-emission-performance-standards-cars-and-vans_en#:~{}:text=The%20Commission%20proposes%20the%20following,%2C%20and%20100%20%25%20for%20vans (accessed on 17 July 2022).
3. Bieker, G. A Global Comparison of the Life-Cycle Greenhouse Gas Emissions of Combustion Engine and Electric Passenger Cars. International Council on Clean Transportation. 2021. Available online: https://theicct.org/publication/a-global-comparison-of-the-life-cycle-greenhouse-gas-emissions-of-combustion-engine-and-electric-passenger-cars/ (accessed on 17 July 2022).
4. Märtz, A.; Plötz, P.; Jochem, P. Global perspective on CO_2 emissions of electric vehicles. *Environ. Res. Lett.* **2021**, *16*, 054043. [CrossRef]
5. European Environmental Agency. *Electric Vehicles from Life Cycle and Circular Economy Perspectives*; European Environmental Agency: Copenhagen, Denmark, 2018. [CrossRef]
6. Statharas, S.; Moysoglou, Y.; Siskos, P.; Zazias, G.; Capros, P. Factors Influencing Electric Vehicle Penetration in the EU by 2030: A Model-Based Policy Assessment. *Energies* **2019**, *12*, 2739. [CrossRef]
7. Blanck, R.; Kasten, P.; Jöhrens, J.; Kräck, J.; Räder, D.; Kräck, J.; Mathieu, L. Plug-in Hybrid Electric Cars: Market Development, Technical Analysis and CO2 Emission Scenarios for Germany. 2020. Available online: https://policycommons.net/artifacts/1572737/plug-in-hybrid-electric-cars/2262516/ (accessed on 17 July 2022).
8. Plötz, P.; Moll, C.; Bieker, G.; Mock, P. From lab-to-road: Real-world fuel consumption and CO_2 emissions of plug-in hybrid electric vehicles. *Environ. Res. Lett.* **2021**, *16*, 054078. [CrossRef]
9. Ktistakis, M.A.; Pavlovic, J.; Fontaras, G. Developing an optimal sampling design to monitor the vehicle fuel consumption gap. *Sci. Total Environ.* **2022**, *832*, 154943. [CrossRef]
10. Tansini, A.; Pavlovic, J.; Fontaras, G. Quantifying the real-world CO_2 emissions and energy consumption of modern plug-in hybrid vehicles. *J. Clean. Prod.* **2022**, *362*, 132191. [CrossRef]
11. Selleri, T.; Melas, A.; Franzetti, J.; Ferrarese, C.; Giechaskiel, B.; Suarez-Bertoa, R. On-Road and Laboratory Emissions from Three Gasoline Plug-in Hybrid Vehicles-Part 1: Regulated and Unregulated Gaseous Pollutants and Green House Gases. *Energies* **2022**, *15*, 2401. [CrossRef]
12. Suarez-Bertoa, R.; Pavlovic, J.; Trentadue, G.; Otura-Garcia, M.; Tansini, A.; Ciuffo, B.; Astorga, C. Effect of Low Ambient Temperature on Emissions and Electric Range of Plug-In Hybrid Electric Vehicles. *ACS Omega* **2019**, *4*, 3159–3168. [CrossRef]
13. Lähde, T.; Giechaskiel, B.; Pavlovic, J.; Suarez-Bertoa, R.; Valverde, V.; Clairotte, M.; Martini, G. Solid particle number emissions of 56 light-duty Euro 5 and Euro 6 vehicles. *J. Aerosol Sci.* **2021**, *159*, 105873. [CrossRef]
14. Giechaskiel, B.; Melas, A.; Martini, G.; Dilara, P. Overview of Vehicle Exhaust Particle Number Regulations. *Processes* **2021**, *9*, 2216. [CrossRef]

15. Giechaskiel, B.; Joshi, A.; Ntziachristos, L.; Dilara, P. European Regulatory Framework and Particulate Matter Emissions of Gasoline Light-Duty Vehicles: A Review. *Catalysts* **2019**, *9*, 586. [CrossRef]
16. McCaffery, C.; Zhu, H.; Li, C.; Durbin, T.D.; Johnson, K.C.; Jung, H.; Brezny, R.; Geller, M.; Karavalakis, G. On-road gaseous and particulate emissions from GDI vehicles with and without gasoline particulate filters (GPFs) using portable emissions measurement systems (PEMS). *Sci. Total Environ.* **2019**, *710*, 136366. [CrossRef] [PubMed]
17. Giechaskiel, B.; Melas, A.; Valverde, V.; Otura, M.; Martini, G. Challenging Conditions for Gasoline Particulate Filters (GPFs). *Catalysts* **2022**, *12*, 70. [CrossRef]
18. Boger, T.; Glasson, T.; Rose, D.; Ingram-Ogunwumi, R.; Wu, H. Next Generation Gasoline Particulate Filters for Uncatalyzed Applications and Lowest Particulate Emissions. *SAE Int. J. Adv. Curr. Pract. Mobil.* **2021**, *3*, 2452–2461. [CrossRef]
19. Dorscheidt, F.; Sterlepper, S.; Görgen, M.; Nijs, M.; Claßen, J.; Yadla, S.K.; Maurer, R.; Pischinger, S.; Krysmon, S.; Abdelkader, A. *Gasoline Particulate Filter Characterization Focusing on the Filtration Efficiency of Nano-Particulates Down to 10 nm*; SAE Technical Paper No. 2020-01-2212; SAE: Warrendale, PA, USA, 2020. [CrossRef]
20. Yu, F.; Zhong, Z.; Wang, Q.; Liao, S.; Zhu, M.; Sha, Q.; Liu, J.; Zheng, J. Characterizing the particle number emissions of light-duty gasoline vehicles under different engine technologies and driving conditions. *Environ. Res.* **2022**, *213*, 113648. [CrossRef]
21. Giechaskiel, B.; Valverde, V.; Kontses, A.; Melas, A.; Martini, G.; Balazs, A.; Andersson, J.; Samaras, Z.; Dilara, P. Particle Number Emissions of a Euro 6d-Temp Gasoline Vehicle under Extreme Temperatures and Driving Conditions. *Catalysts* **2021**, *11*, 607. [CrossRef]
22. Yang, Z.; Ge, Y.; Thomas, D.; Wang, X.; Su, S.; Li, H.; He, H. Real driving particle number (PN) emissions from China-6 compliant PFI and GDI hybrid electrical vehicles. *Atmos. Environ.* **2018**, *199*, 70–79. [CrossRef]
23. Wang, Y.; Wang, J.; Hao, C.; Wang, X.; Li, Q.; Zhai, J.; Ge, Y.; Hao, L.; Tan, J. Characteristics of instantaneous particle number (PN) emissions from hybrid electric vehicles under the real-world driving conditions. *Fuel* **2020**, *286*, 119466. [CrossRef]
24. Conger, M.; Holmén, B.A. Characterization of Real-World Particle Number Emissions during Reignition Events from a 2010 Light-Duty Hybrid Electric Vehicle. *Transp. Res. Rec. J. Transp. Res. Board* **2015**, *2503*, 137–146. [CrossRef]
25. Choi, Y.; Yi, H.; Oh, Y.; Park, S. Effects of engine restart strategy on particle number emissions from a hybrid electric vehicle equipped with a gasoline direct injection engine. *Atmos. Environ.* **2021**, *253*, 118359. [CrossRef]
26. Feinauer, M.; Ehrenberger, S.; Epple, F.; Schripp, T.; Grein, T. Investigating Particulate and Nitrogen Oxides Emissions of a Plug-In Hybrid Electric Vehicle for a Real-World Driving Scenario. *Appl. Sci.* **2022**, *12*, 1404. [CrossRef]
27. Fan, Q.; Wang, Y.; Xiao, J.; Wang, Z.; Li, W.; Jia, T.; Zheng, B.; Taylor, R. *Effect of Oil Viscosity and Driving Mode on Oil Dilution and Transient Emissions Including Particle Number in Plug-In Hybrid Electric Vehicle*; SAE Technical Paper No. 2020-01-0362; SAE: Warrendale, PA, USA, 2020. [CrossRef]
28. Zhang, J.; Richter, J.-M.; Kaczmarek, C. *Catalysts for Post Euro 6 Plug-In Hybrid Electric Vehicles*; SAE Technical Paper No. 2020-01-0354; SAE: Warrendale, PA, USA, 2020. [CrossRef]
29. Zhang, L.; He, S.; Zhang, Q.; Liao, Y.; Zhang, H. *Gasoline Particulate Filter Applications for Plug-In Hybrid and Traditional Cars*; SAE Technical Paper No. 2020-01-1430; SAE: Warrendale, PA, USA, 2020. [CrossRef]
30. Giakoumis, E.G.; Zachiotis, A.T. Investigation of a Diesel-Engined Vehicle's Performance and Emissions during the WLTC Driving Cycle—Comparison with the NEDC. *Energies* **2017**, *10*, 240. [CrossRef]
31. Giechaskiel, B.; Cresnoverh, M.; Jörgl, H.; Bergmann, A. Calibration and accuracy of a particle number measurement system. *Meas. Sci. Technol.* **2010**, *21*, 045102. [CrossRef]
32. Yamada, H.; Funato, K.; Sakurai, H. Application of the PMP methodology to the measurement of sub-23 nm solid particles: Calibration procedures, experimental uncertainties, and data correction methods. *J. Aerosol Sci.* **2015**, *88*, 58–71. [CrossRef]
33. Giechaskiel, B.; Lähde, T.; Melas, A.D.; Valverde, V.; Clairotte, M. Uncertainty of laboratory and portable solid particle number systems for regulatory measurements of vehicle emissions. *Environ. Res.* **2021**, *197*, 111068. [CrossRef]
34. Bonnel, P.; Clairotte, M.; Cotogno, G.; Gruening, C.; Loos, R.; Manara, D.; Melas, A.; Selleri, T.; Tutuianu, M.; Valverdre, V.; et al. *European Market Surveillance of Motor Vehicles*; Publication Office of the European Union: Luxembourg, 2022. [CrossRef]
35. Giechaskiel, B.; Riccobono, F.; Vlachos, T.; Mendoza-Villafuerte, P.; Suarez-Bertoa, R.; Fontaras, G.; Bonnel, P.; Weiss, M. Vehicle Emission Factors of Solid Nanoparticles in the Laboratory and on the Road Using Portable Emission Measurement Systems (PEMS). *Front. Environ. Sci.* **2015**, *3*, 82. [CrossRef]
36. Berthome, V.; Chalet, D.; Hetet, J.-F. Characterization of Particle Emissions of Turbocharged Direct Injection Gasoline Engine in Transients and Hot Start Conditions. *J. Therm. Sci.* **2021**, *30*, 2056–2070. [CrossRef]
37. Samaras, Z.; Rieker, M.; Papaioannou, E.; van Dorp, W.; Kousoulidou, M.; Ntziachristos, L.; Andersson, J.; Bergmann, A.; Hausberger, S.; Keskinen, J.; et al. Perspectives for regulating 10 nm particle number emissions based on novel measurement methodologies. *J. Aerosol Sci.* **2022**, *162*, 105957. [CrossRef]